Published in final edited form as:
Circ Cardiovasc Imaging. 2010 May ; 3(3): 290–297. doi:10.1161/CIRCIMAGING.109.911313.

High prevalence of Left Ventricular Regional Dysfunction in Arrhythmogenic Right Ventricular Dysplasia: a tagged MRI study

Aditya Jain, MD, MPH[1], **Monda L. Shehata, MD**[1], **Matthias Stuber, PhD**[1], **Seth J. Berkowitz, MD**[1], **Hugh Calkins, MD**[2], **Joao A. C. Lima, MD**[1,2], **David A. Bluemke, MD, PhD**[1,2,3], and **Harikrishna Tandri, MD**[2]

[1]Department of Radiology, Johns Hopkins University School of Medicine, MD, USA

[2]Division of Cardiology, Johns Hopkins University School of Medicine, MD, USA

[3]Radiology and Imaging Sciences, National Institutes of Health, MD, USA

Abstract

Background—Although arrhythmogenic right ventricular dysplasia (ARVD) is characterized by predominantly right sided morphologic changes, genetic/histological and molecular changes are biventricular. Alterations in regional left ventricular (LV) strain in patients referred for suspicion of ARVD have not previously been determined.

Methods and Results—The study population included 21 patients with suspected ARVD who underwent evaluation with MRI including tagging. Eleven healthy volunteers served as controls. Global RV and LV function were studied by MRI and peak regional systolic circumferential strain (Ecc, %) was calculated by harmonic phase from tagged MRI based on a 16-segment model. Patients who met ARVD Task Force criteria were classified as definite ARVD, whereas patients with a positive family history who had one additional minor criterion and patients without a family history with at least 1 major or 2 minor criteria were classified as probable ARVD.

Of the 21 ARVD subjects, 11 had definite ARVD (63.6% males, mean age 41.2 ± 14.2 years) and, 10 had probable ARVD (30% males, 34.9 ± 12.1 years). Compared with controls (58.9 ± 6.2%), probable ARVD patients (53.6 ± 7.6%) had similar global RV ejection fraction (RVEF) ($p > 0.05$), but definite ARVD patients (45.2 ± 6.0%) had significantly reduced RVEF ($p < 0.0001$). Global LVEF was normal in all three groups ($p > 0.05$). Compared to controls, mean LV circumferential strain (Ecc) was significantly reduced in 7/16 (44%) segments in definite ARVD, and 3/16 segments (19%) in probable ARVD ($p < 0.05$ for all).

Conclusions—There was a high prevalence of regional LV dysfunction in patients with definite ARVD, with less dysfunction in those with probable ARVD. Further, the extent of regional LV dysfunction appeared to parallel RV dysfunction, whereas global LV function was normal. Similar to the RV abnormalities, our findings suggest ARVD results in regional alterations of LV dysfunction prior to global abnormalities.

Keywords

ARVD; LV involvement; tagging; regional strain

Address for correspondence: Harikrishna Tandri, MD, Carnegie 568, The Johns Hopkins Hospital, 600 North Wolfe Street, Baltimore, MD, 21287, Phone: 410-903-1182, Fax: 410-502-9148, htandri1@jhmi.edu.

Introduction

Arrhythmogenic right ventricle dysplasia (ARVD) is a familial cardiomyopathy that is characterized by predominant right ventricular (RV) dysfunction, and histologically by myocyte loss and fibro-fatty infiltration of the myocardium [1]. Defective cell-to cell adhesion due to mutations in genes encoding desmosomal proteins have been implicated in the pathogenesis of ARVD. The result is disruption of the cardiac gap junction apparatus, which has been thought to result both in the functional impairment and the failure of impulse transmission with subsequent arrhythmogenesis. The ultrastructural and molecular consequences are expressed in both ventricles alike, and this has promoted the notion that ARVD is a biventricular cardiomyopathy, with predominant involvement of the thin-walled right ventricle [1].

Patients with end-stage or advanced ARVD are observed with clinically obvious biventricular dysfunction that can be readily identified using echocardiography or MRI. When present, left ventricular (LV) dysfunction is often associated with significantly more adverse clinical outcomes such as ventricular arrhythmias and heart failure [4, 5]. LV contraction abnormalities have been demonstrated in ARVD in association with advanced RV disease by previous imaging studies using radionuclide angiography [6, 7], echocardiography [8, 9] and electron-beam computed tomography [10]. More recently, ARVD with dominant LV involvement has also been reported in the United Kingdom, [2, 3] but not yet in the United States.

Regional contraction abnormalities often precede global dysfunction but have not previously been quantified using myocardial strain analysis for the RV or LV for ARVD. Unfortunately the thin wall of the RV makes regional motion tracking extremely challenging. However, tagged cardiovascular magnetic resonance imaging (MRI) of the heart provides objective measurements of regional LV function [11] with great precision and reliability [12]. The purpose of this study was to quantify regional LV function in patients with high clinical suspicion for ARVD using tagged MRI.

Methods

The study population included 21 patients who were evaluated for ARVD at the Johns Hopkins ARVD program following a positive family history (n=13, 62%) or left bundle branch block morphology ventricular tachycardia (n=8, 38%). All of these patients underwent initial non-invasive testing according to a standardized protocol including an electrocardiogram (ECG), signal-averaged electrocardiogram (SAECG), Holter monitoring, echocardiogram, exercise testing, and cardiac MRI. They underwent further invasive testing at the discretion of the cardiologist which included electrophysiologic study, RV angiography, and endomyocardial biopsy. 11 healthy volunteers served as controls. Diagnosis of ARVD was established based on the criteria set by the Task Force of the Working Group of Myocardial and Pericardial Disease of the European Society of Cardiology and of the Scientific Council on Cardiomyopathies of the International Society and Federation of Cardiology [13]. Among those who did not meet the Task Force criteria, patients with a positive family history who had one additional minor criterion and patients without a family history with at least have 1 major or 2 minor criteria were classified as probable ARVD.

MR Imaging Protocol

MR images of study subjects were obtained on 1.5-T scanners (CV/I, GE Medical Systems, Waukesha, WI or Philips Medical Systems, Best, The Netherlands) at the Johns Hopkins Hospital and included both fast spin-echo (FSE) and gradient-echo sequences. Fat-

suppressed and non fat-suppressed FSE sequences were acquired in the axial and short-axis planes with breath-hold double-inversion recovery blood suppression pulses with repetition time (TR) of 1 or 2 R-R intervals, time to excitation (TE) of 10-20 ms, slice thickness of 5-10 mm and slice gap of 2-5 mm. The matrix and field of view (FOV) were 256 × 256 and 24-36 cm, respectively. Cine functional images were obtained in the axial and short-axis planes using breath-hold steady state free precession (SSFP) imaging. The flip angle was 40-60 degrees and TE was set to minimum. For SSFP imaging, the slice thickness was 5-8 mm with a slice gap of 2-6 mm. The matrix and FOV were 256 × 160 and 36-40 cm, respectively. Following this, inversion recovery prepared breath-hold 2D cine gradient-echo images were obtained 20 minutes after contrast agent injection [0.2 mmol/kg of gadodiamide (Omniscan, Amersham Health, Princeton, New Jersey)]. Imaging parameters included TR/TE, 7.2/3.2; inversion time optimized, 150-250 ms; flip angle, 25 degrees; slice thickness, 8 mm; slice gap, 2 mm; number of excitations, 2; matrix, 256 × 192; and FOV, 360 × 270 mm. 2D myocardial delayed enhancement (MDE) MRI scans were obtained in the short axis and axial planes at 10 mm intervals covering the entire right and left ventricles. All studies used a phased array surface coil for signal reception. The temporal resolution of the cine images was less than or equal to 50 ms.

Tagging protocol

After completing the standard imaging protocol, three tagged short axis slices (base to apex) were obtained. Parallel striped tags were prescribed in two orthogonal orientations (0° and 90°) using ECG-triggered fast gradient-echo sequence with spatial modulation of magnetization [14, 15] and were superimposed as grid images (Figure 1). The parameters for tagged MR images were FOV, 40 cm; slice thickness, 8-10 mm; TR, 3.5-7.2 ms; echo time, 2.0-4.2 ms; flip angle, 10–12 degrees; matrix size, 256 × 96 to 140; temporal resolution, 20-40 ms and tag spacing, 7 mm.

MR image analysis

MR images were assessed by experienced cardiac MRI readers at the Johns Hopkins Hospital who were blinded to all clinical and other diagnostic information. MR images were transferred to an Advantage windows workstation (GE Medical Systems, Waukesha, WI) for analysis. Quantitative analysis was performed using dedicated commercially available MASS software program (Medis, Leiden, The Netherlands). This software was used to view images using standardized window width and level settings. The first image after the R wave trigger represented the end diastolic image. End systolic image was defined visually as the one with the smallest ventricular cavity size. Quantitative MR parameters included end-diastolic volume (EDV), end-systolic volume (ESV) and ejection fraction (EF) for both ventricles. Diastolic and systolic ventricular volume measurements were obtained by summation of planimetered areas obtained from serial short axis images. The MR images were qualitatively assessed for ventricular enlargement, global hypokinesis, regional wall motion abnormalities, fat, delayed enhancement and aneurysms.

Strain analysis

Short-axis tagged slices were analyzed for peak mid-wall regional systolic circumferential strain (Ecc) by the HARP method (Harmonic Phase, Diagnosoft, Palo Alto, California, USA) [16, 17] based on the 16-segment heart model [18]. LV was divided into 3 circular basal, mid-cavity and apical short-axis slices perpendicular to the long axis of the heart. With regard to the circumferential location, the basal and mid-cavity slices were divided into 6 segments of 60 degrees each -- *anterior, anteroseptal, inferoseptal, inferior, inferolateral and lateral* and the apical slice was divided into 4 segments of 90 degrees each – *anterior, septal, inferior and lateral*. By convention, since Ecc relates to systolic circumferential shortening, their value during systole is negative and a more negative value reflects

enhanced contraction. One of our previous studies has shown excellent inter- and intra-observer agreement for peak systolic mid-wall Ecc (correlation coefficient > 0.8, for both) in myocardial MR-tagged image analysis using the HARP technique [19].

Statistical Analysis

All continuous variables were reported as mean ± SD, except strain which was expressed in %. All categorical variables were reported as frequency (%). Continuous variables were compared among different subgroups of study subjects by Mann-Whitney test. Categorical variables were compared using Fisher's exact test. Two-tailed p-value less than 0.05 was considered statistically significant. Statistical analyses were performed in STATA statistical software (Version 9.0, College Station, TX).

Results

Baseline characteristics

Table 1 describes the demographics, electrophysiologic and structural abnormalities of the study population which was composed of 21 patients with ARVD and 11 controls. Out of the 21 patients with ARVD, 11 (52%) were classified as having definite ARVD and 10 (48%) as probable ARVD. Among the definite ARVD group, 45% patients fulfilled 4 Task Force criteria points, and remaining 55% fulfilled more than 4. Among the probable ARVD group, 20% patients satisfied 2, and remaining 80% patients satisfied 3 points. The mean age of the definite ARVD and probable ARVD patients was 41.2 ± 14.2 and 34.9 ± 12.1 years ($p>0.05$), and 7 (64%) and 3 (30%) were men respectively ($p>0.05$). The presence of greater than 1000 premature ventricular contractions on a 24-hour Holter monitor and echocardiographic evidence of varying degrees of RV functional impairment was significantly more often seen in definite ARVD group as compared to probable ARVD group ($p< 0.05$ for both). The mean age of controls was 29.8 ± 6.7 years and 6 (55%) were men. None of the controls had any prior symptoms, family history, electrical or structural abnormalities consistent with ARVD.

Characteristics of RV and LV on MRI

Shown in Table 2 are the detailed MRI findings of individuals included in the study. While definite ARVD patients in general demonstrated a higher degree of RV structural abnormalities on MRI, they showed a significantly higher presence of varying degrees of dilatation and delayed enhancement of the RV as compared to patients with probable ARVD (all $p< 0.05$). Global RV volumes were significantly higher for both definite and probable ARVD patients as compared to controls (all $p< 0.05$). RVEF in definite ARVD was significantly lower relative to probable ARVD ($p= 0.01$) as well as controls ($p< 0.001$). Early ARVD patients appeared to be have a preserved RVEF with respect to controls ($p>0.05$).

Among the definite ARVD group, the most commonly seen LV abnormality was intra myocardial fat (3/11, 27%), followed by regional wall motion defects (2/11, 18%), dilatation (1/11, 9%) and delayed enhancement (1/11, 9%). Similarly, among the probable ARVD group, the LV abnormalities observed were intra myocardial fat (1/10, 10%) and delayed enhancement (1/10, 10%). Quantitatively, global LV volumes and LVEF in patients with definite and probable ARVD were similar to controls (all p= NS).

Regional LV systolic function

Shown in Table 3 are mean circumferential strain values in the study population for the individual myocardial segments derived from 16-segment model. Patients with definite ARVD revealed significantly lower mean Ecc than controls in basal inferior (-13.2% vs.

-17.3%, p= 0.01), basal inferolateral (-18.5% vs.-20.7%, p= 0.03), basal lateral (-17.2% vs. -21.2%, p< 0.01), mid inferior (-13.5% vs. -19.8%, p< 0.01), mid inferolateral (-19.3% vs. -22.1%, p< 0.001), mid lateral (-19.3% vs. -23.0%, p< 0.01) and apical lateral (-18.8% vs. -23.4%, p< 0.01) segments, respectively. Mean Ecc was significantly lower in probable ARVD compared to controls in basal lateral (-17.6% vs. -21.2%, p= 0.01), mid lateral (-18.2% vs. -23.0%, p< 0.01) and apical lateral (-18.2% vs. -23.4%, p= 0.02) segments, respectively.

Figure 2a shows mean Ecc according to the study groups among myocardial regions along the longitudinal axis of the heart. Definite ARVD patients demonstrated reduced strain in all 3 regions in contrast to controls – base, mid-cavity and apex (-15.7% vs. -18.9%, p< 0.01; -17.5% vs. -20.3%, p< 0.01; -17.6% vs. -20.7%, p= 0.02 respectively) whereas probable ARVD group showed reduced strain only in mid-cavity region (-18.3% vs. -20.3%, p= 0.04).

Figure 2b depicts distribution of mean Ecc circumferentially around the heart in the study population. Of the anterior, septal, inferior and lateral walls, definite ARVD reported a reduced strain in all of them compared to controls (-16.7% vs. -19.7%, p< 0.01; -16.9% vs. -18.7%, p= 0.04; -13.8% vs. -18.7%, p< 0.01; -18.6% vs. -22.1%, p< 0.001 respectively) (Figure 1). This is in contrast to probable ARVD which showed reduced strain in lateral wall alone (-18.2% vs. -22.1%, p<0.01).

Discussion

To our knowledge, this is the first study to quantitatively assess regional LV function in ARVD using strain analysis. This approach revealed regional LV systolic dysfunction despite a preserved global LV function. Further, the extent of LV dysfunction appeared to parallel RV dysfunction with definite ARVD showing worse LV regional dysfunction.

Probable ARVD

Patients with a strong clinical suspicion of ARVD but satisfying less than the required number of Task Force criteria for the definite diagnosis of the disease were considered to have probable ARVD. Probable ARVD may represent an early spectrum of the disease with possible progression to diagnostically more overt forms with time. In a high risk population (such as positive mutation carrier status or positive family history), the classification of probable ARVD may be particularly relevant. Such patients may do not fulfill traditional ARVD criteria, but may have a higher pre-test probably probability for disease. Thus, in our practice, such patients frequently mandate closer clinical follow-up if several, but not all ARVD criteria are fulfilled.

Left ventricular involvement in ARVD

Left-sided involvement in ARVD has been described, but it is frequently considered a late manifestation of advanced disease [20, 21]. However, the recent and important advances in the field of genetic characterization of the disease led to the hypothesis of a potential LV affliction in ARVD from its early stages [3]. Most disease-causing mutations have been found to involve genes encoding different component proteins of the cardiac desmosome such as desmoplakin, plakophilin-2, junctional plakoglobin, desmoglein-2 and desmocollin-2 [1]. Although different mutations may impact ventricles differentially [3], the spectrum of their phenotypic expression should involve both ventricles concomitantly as right and left side of the heart are similar with respect to desmosomal structure and gene expression. Our findings are plausible with the purported common genetic substrate between the two ventricles, support the emerging evidence in favor of LV involvement early along the natural history of

the disease and favor the need of a contemporaneous revision of Task Force criteria to include LV descriptions [3, 22].

With respect to qualitative changes, LV functional abnormalities in ARVD have been previously reported [1, 10, 23]. However, a systematic regional quantification of LV contractile function in context to global function in ARVD has not been previously undertaken. Using myocardial tagging, we discovered decreased regional LV contraction in probable ARVD that had a higher prevalence in definite ARVD. The lateral wall showed a predilection for reduced strain in probable ARVD patients while definite disease additionally involved the anterior, septal and inferior walls. Similarly, reduced strain noted first in the mid-cavity region of the LV seemed to progress to basal and apical regions with increase in disease severity. These subclinical reductions in regional LV contractility as demonstrated by reduced systolic circumferential shortening showed a positive correlation with increasing RV impairment and existed without significant morphological abnormalities of the LV in the context of normal global LV function. Regional contraction derangement appears to be a more sensitive indicator of LV involvement, and this may be of great relevance in the classic disease paradigm where the RV is consistently more severely affected than the LV and conspicuous signs of LV involvement may not set in until later in the course of the disease [2, 3].

Prognostic significance of LV involvement

The “left-sidedness” of ARVD is known to portent an increased likelihood of an eventful clinical course. Prospective and retrospective studies have highlighted LV involvement to be associated with an increased risk of palpitations, syncopal episodes, potentially lethal arrhythmias and heart failure than isolated RV disease alone, which explains why LV involvement can help in identifying those ARVD patients who would benefit the most from timely ICD placement [4, 5]. In the light of the aforementioned, the interpretation of the findings of our study of a possible LV involvement in ARVD in the form of a subclinical reduction in myocardial contraction may be critical from the prognostic stand-point.

Study strengths and limitations

Strengths of this study include non-subjective analysis of regional LV function by the novel application of myocardial tagging in ARVD, comparative assessment of probable and definite ARVD patients against normals, and cardiac MRI scanning for qualitative and quantitative evaluation of ARVD. While the inclusion of individuals who do not fulfill adequate number of Task Force criteria may imply inclusion of early ARVD patients, it could also lead to a loss of specificity and admittance of false-positive patients with similar disorders such as idiopathic ventricular tachycardia and other types of cardiomyopathies. Our study groups had variable age and gender distribution which may have affected the strain results. However, there are no population-based studies demonstrating the variability of strain patterns by age or gender. Because of the cross-sectional nature of our study, temporal trends in LV involvement and disease progression in probable ARVD patients over time could not be addressed. The study sample size is small and the results should be validated in a large-scale genotyped cohort of ARVD patients.

Clinical implications

These results support the current molecular/genetic basis of ARVD with biventricular disease expression, even early in the course of the disease. This study shows the ability of MRI tagging to measure myocardial strain in ARVD populations, and as a sensitive method for detecting regional contraction abnormalities in an ARVD population free of global LV functional deficits. Abnormal strain measurements may be the first indication of an incipient overt LV dysfunction, warranting closer clinical follow-up and surveillance. It remains to be

seen whether these subclinical alterations in LV systolic function independently confer any increased risk of adverse clinical outcomes in ARVD.

Acknowledgments

The Johns Hopkins ARVD Program is supported by the Bogle Foundation, the Campanella family, the Wilmerding Endowment, and the National Institutes of Health research grant 1 UO1 HL65594-01A1. The authors are grateful to ARVD patients and families who have made this work possible.

References

1. Jain A, Tandri H, Calkins H, Bluemke DA. Role of cardiovascular magnetic resonance imaging in arrhythmogenic right ventricular dysplasia. J Cardiovasc Magn Reson 2008;10(1):32. [PubMed: 18570661]
2. Sen-Chowdhry S, Syrris P, Prasad SK, Hughes SE, Merrifield R, Ward D, Pennell DJ, McKenna WJ. Left-dominant arrhythmogenic cardiomyopathy: an under-recognized clinical entity. J Am Coll Cardiol Dec 16;2008 52(25):2175–2187. [PubMed: 19095136]
3. Sen-Chowdhry S, Syrris P, Ward D, Asimaki A, Sevdalis E, McKenna WJ. Clinical and genetic characterization of families with arrhythmogenic right ventricular dysplasia/cardiomyopathy provides novel insights into patterns of disease expression. Circulation Apr 3;2007 115(13):1710–1720. [PubMed: 17372169]
4. Corrado D, Leoni L, Link MS, Della Bella P, Gaita F, Curnis A, Salerno JU, Igidbashian D, Raviele A, Disertori M, Zanotto G, Verlato R, Vergara G, Delise P, Turrini P, Basso C, Naccarella F, Maddalena F, Estes NA 3rd, Buja G, Thiene G. Implantable cardioverter-defibrillator therapy for prevention of sudden death in patients with arrhythmogenic right ventricular cardiomyopathy/dysplasia. Circulation Dec 23;2003 108(25):3084–3091. [PubMed: 14638546]
5. Corrado D, Basso C, Thiene G, McKenna WJ, Davies MJ, Fontaliran F, Nava A, Silvestri F, Blomstrom-Lundqvist C, Wlodarska EK, Fontaine G, Camerini F. Spectrum of clinicopathologic manifestations of arrhythmogenic right ventricular cardiomyopathy/dysplasia: a multicenter study. J Am Coll Cardiol Nov 15;1997 30(6):1512–1520. [PubMed: 9362410]
6. Peters S, Reil GH. Risk factors of cardiac arrest in arrhythmogenic right ventricular dysplasia. Eur Heart J Jan;1995 16(1):77–80. [PubMed: 7737226]
7. Horimoto M, Akino M, Takenaka T, Igarashi K, Inoue H, Kawakami Y. Evolution of left ventricular involvement in arrhythmogenic right ventricular cardiomyopathy. Cardiology 2000;93(3):197–200. [PubMed: 10965092]
8. Pinamonti B, Sinagra G, Salvi A, Di Lenarda A, Morgera T, Silvestri F, Bussani R, Camerini F. Left ventricular involvement in right ventricular dysplasia. Am Heart J Mar;1992 123(3):711–724. [PubMed: 1539522]
9. Lindstrom L, Nylander E, Larsson H, Wranne B. Left ventricular involvement in arrhythmogenic right ventricular cardiomyopathy - a scintigraphic and echocardiographic study. Clin Physiol Funct Imaging May;2005 25(3):171–177. [PubMed: 15888098]
10. Tada H, Shimizu W, Ohe T, Hamada S, Kurita T, Aihara N, Kamakura S, Takamiya M, Shimomura K. Usefulness of electron-beam computed tomography in arrhythmogenic right ventricular dysplasia. Relationship to electrophysiological abnormalities and left ventricular involvement. Circulation Aug 1;1996 94(3):437–444. [PubMed: 8759086]
11. Zerhouni EA, Parish DM, Rogers WJ, Yang A, Shapiro EP. Human heart: tagging with MR imaging--a method for noninvasive assessment of myocardial motion. Radiology Oct;1988 169(1): 59–63. [PubMed: 3420283]
12. Castillo E, Lima JA, Bluemke DA. Regional myocardial function: advances in MR imaging and analysis. Radiographics Oct;2003 23:S127–140. Spec No. [PubMed: 14557507]
13. McKenna WJ, Thiene G, Nava A, Fontaliran F, Blomstrom-Lundqvist C, Fontaine G, Camerini F. Diagnosis of arrhythmogenic right ventricular dysplasia/cardiomyopathy. Task Force of the Working Group Myocardial and Pericardial Disease of the European Society of Cardiology and of the Scientific Council on Cardiomyopathies of the International Society and Federation of Cardiology. Br Heart J Mar;1994 71(3):215–218. [PubMed: 8142187]

14. Axel L, Dougherty L. MR imaging of motion with spatial modulation of magnetization. Radiology Jun;1989 171(3):841–845. [PubMed: 2717762]
15. Ibrahim el SH, Stuber M, Schar M, Osman NF. Improved myocardial tagging contrast in cine balanced SSFP images. J Magn Reson Imaging Nov;2006 24(5):1159–1167. [PubMed: 17031834]
16. Osman NF, Prince JL. Regenerating MR tagged images using harmonic phase (HARP) methods. IEEE Trans Biomed Eng Aug;2004 51(8):1428–1433. [PubMed: 15311829]
17. Sampath S, Derbyshire JA, Atalar E, Osman NF, Prince JL. Real-time imaging of two-dimensional cardiac strain using a harmonic phase magnetic resonance imaging (HARP-MRI) pulse sequence. Magn Reson Med Jul;2003 50(1):154–163. [PubMed: 12815690]
18. Cerqueira MD, Weissman NJ, Dilsizian V, Jacobs AK, Kaul S, Laskey WK, Pennell DJ, Rumberger JA, Ryan T, Verani MS. Standardized myocardial segmentation and nomenclature for tomographic imaging of the heart: a statement for healthcare professionals from the Cardiac Imaging Committee of the Council on Clinical Cardiology of the American Heart Association. Circulation Jan 29;2002 105(4):539–542. [PubMed: 11815441]
19. Castillo E, Osman NF, Rosen BD, El-Shehaby I, Pan L, Jerosch-Herold M, Lai S, Bluemke DA, Lima JA. Quantitative assessment of regional myocardial function with MR-tagging in a multi-center study: interobserver and intraobserver agreement of fast strain analysis with Harmonic Phase (HARP) MRI. J Cardiovasc Magn Reson 2005;7(5):783–791. [PubMed: 16358393]
20. Hulot JS, Jouven X, Empana JP, Frank R, Fontaine G. Natural history and risk stratification of arrhythmogenic right ventricular dysplasia/cardiomyopathy. Circulation Oct 5;2004 110(14): 1879–1884. [PubMed: 15451782]
21. Dalal D, Nasir K, Bomma C, Prakasa K, Tandri H, Piccini J, Roguin A, Tichnell C, James C, Russell SD, Judge DP, Abraham T, Spevak PJ, Bluemke DA, Calkins H. Arrhythmogenic right ventricular dysplasia: a United States experience. Circulation Dec 20;2005 112(25):3823–3832. [PubMed: 16344387]
22. Dalal D, Tandri H, Judge DP, Amat N, Macedo R, Jain R, Tichnell C, Daly A, James C, Russell SD, Abraham T, Bluemke DA, Calkins H. Morphologic variants of familial arrhythmogenic right ventricular dysplasia/cardiomyopathy a genetics-magnetic resonance imaging correlation study. J Am Coll Cardiol Apr 14;2009 53(15):1289–1299. [PubMed: 19358943]
23. Bomma C, Dalal D, Tandri H, Prakasa K, Nasir K, Roguin A, Tichnell C, James C, Lima JA, Calkins H, Bluemke DA. Regional differences in systolic and diastolic function in arrhythmogenic right ventricular dysplasia/cardiomyopathy using magnetic resonance imaging. Am J Cardiol Jun 15;2005 95(12):1507–1511. [PubMed: 15950585]

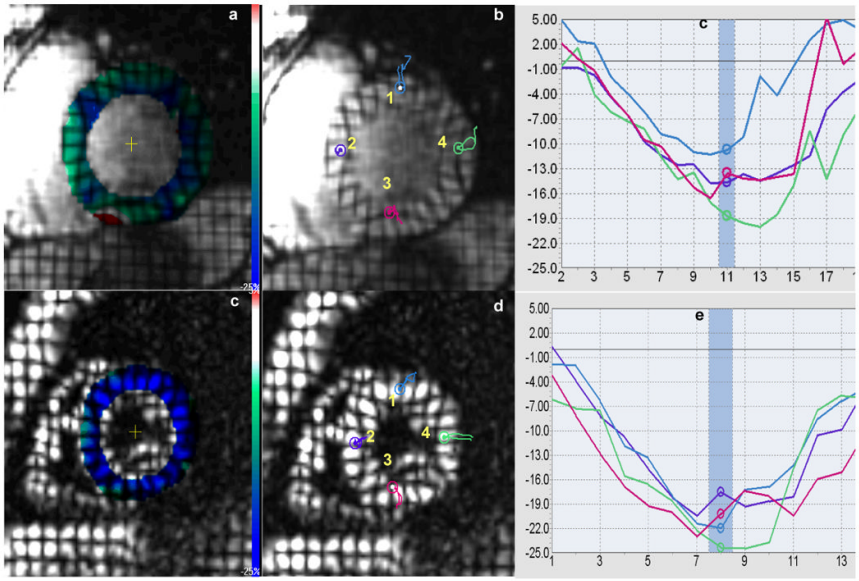

Figure 1.

Figures a and d show color-coded maps superimposed on tagged MR short-axis images from one patient with definite ARVD and healthy control. Bar color demonstrates the spectrum in change of cardiac systolic function: blue color identifies normal contractile state and red color represents dysfunctional areas. The green-dominant myocardium of the ARVD patient indicates generalized weaker systolic function in contrast to the blue-dominant myocardium in the healthy control. Figures b and e show colored probe points inserted each at 1) anterior wall 2) septal wall 3) inferior wall and 4) lateral wall in the patient and control, with figures c and f depicting midwall Ecc plots at the corresponding points. Note decreased Ecc in all four walls in the ARVD patient as compared to the control.

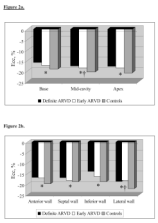

Figure 2.

Figure a shows the distribution of mean Ecc in basal, mid-cavity and apical regions of the heart across the study population. * $p < 0.05$ for comparison of mean Ecc between definite ARVD and controls and † $p < 0.05$ for comparison between probable ARVD and controls. In a similar way, Figure b shows mean Ecc in anterior, septal, inferior and lateral walls. * $p < 0.05$ for comparison of mean Ecc between definite ARVD and controls and † $p < 0.05$ for comparison between probable ARVD and controls.

Table 1
Demographics of the Study Population

Variable	Definite ARVD (n=11)	Probable ARVD (n=10)	Controls (n=11)
Age, years	41.2 ± 14.2	34.9 ± 12.1	29.8 ± 6.7
Men, %	63.6	30.0	54.5
Prior symptoms, %			
Presyncope/Syncope	4 (36)	6 (60)	0 (0)
Palpitation	5 (45)	7 (70)	0 (0)
Family history, %			
SCD < 35 years of age	1 (9)	3 (33)	0 (0)
ARVD by TFC	2 (18)	4 (40)	0 (0)
ARVD by HP evidence	4 (36)	2 (20)	0 (0)
Depolarization, %			
Abnormal SAECG	8 (73)	5 (50)	0 (0)
Epsilon wave	1 (9)	0 (0)	0 (0)
T wave inversions, %			
Beyond V1	8 (73)	4 (40)	0 (0)
Beyond V2	5 (45)	3 (30)	0 (0)
Incomplete RBBB	0	3 (30)	0 (0)
Complete RBBB	0	0 (0)	0 (0)
Arrhythmia, %			
> 1000 PVCs on a 24-hour Holter monitor*	7 (64)	0 (0)	0 (0)
LBBB type VT	4 (36)	3 (30)	0 (0)
Structural abnormalities on Echo, %			
Global RV dilatation	8 (73)	4 (50)	0 (0)
Impaired RV function*	6 (55)	1 (13)	0 (0)
RV wall motion abnormalities	1 (9)	0 (0)	0 (0)
Global LV dilatation	1 (9)	0 (0)	0 (0)
Impaired RV function	0 (0)	0 (0)	0 (0)
Criteria points for ARVD diagnosis			
4+	6 (55)	0 (0)	0 (0)
4	5 (45)	0 (0)	0 (0)
3	0 (0)	8 (80)	0 (0)
2	0 (0)	2 (20)	0 (0)
1	0 (0)	0 (0)	0 (0)

Values are expressed as n (%) or mean ± SD. Among those who did not meet the Task Force criteria, patients with a positive family history who had one additional minor criterion and patients without a family history with atleast 1 major or 2 minor criteria were classified as probable ARVD. Criteria points were calculated by adding the major (2 points each) and minor (1 point each) criteria fulfilled by the individual. The presence of 4 or more points is indicative of arrhythmogenic right ventricular dysplasia (ARVD) diagnosis by Task Force criteria.

* $p<0.05$ for comparison between definite ARVD and probable ARVD patients.

SCD, sudden cardiac death; TFC: Task Force criteria; HP: histopathological; SAECG: signal-averaged ECG; RBBB: right bundle branch block; LBBB: left bundle branch block; VT: ventricular tachycardia

Table 2
Global and Regional Characteristics of the Right and Left Ventricles on MRI

Variable	Definite ARVD (n=11)	Probable ARVD (n=10)	Controls (n=11)
Right Ventricle			
Qualitative parameters, %			
Dilatation*	11 (100)	3 (30)	0 (0)
Aneurysm	2 (18)	2 (20)	0 (0)
Global hypokinesis	6 (55)	2 (20)	0 (0)
Regional hypokinesis/akinesis/dyskinesis	8 (73)	3 (30)	0 (0)
Intramyocardial fat	4 (36)	1 (10)	0 (0)
Delayed enhancement*	7 (64)	1 (10)	0 (0)
Quantitative parameters, ml			
End diastolic volume	213.8 ± 57.6	182.9 ± 61.9	129.5 ± 23.5
End systolic volume	117.9 ± 40.6	88.5 ± 41.7	53.5 ± 14.2
Ejection fraction	45.2 ± 6.0	53.5 ± 7.6	58.9 ± 6.2
Left ventricle			
Qualitative parameters, %			
Dilatation	1 (9)	0 (0)	0 (0)
Aneurysm	0 (0)	0 (0)	0 (0)
Global hypokinesis	0 (0)	0 (0)	0 (0)
Regional hypokinesis/akinesis/dyskinesis	2 (18)	0 (0)	0 (0)
Intramyocardial fat	3 (27)	1 (10)	0 (0)
Delayed enhancement	1 (9)	1 (10)	0 (0)
Quantitative parameters, ml			
End diastolic volume	165.1 ± 52.7	140.8 ± 27.1	125.2 ± 21.5
End systolic volume	63.8 ± 27.1	49.9 ± 12.3	48.2 ± 13.3
Ejection fraction	62.8 ± 4.6	64.7 ± 4.3	61.7 ± 6.6

Values are expressed as n(%) or mean ± SD

* $p < 0.05$ for comparison between definite ARVD and probable ARVD patients

Table 3

Mean circumferential strain values (Ecc, %) in study population for myocardial segments based on the 16-segment heart model

Segment	Definite ARVD (n=11)	Probable ARVD (n=10)	Controls (n=11)	P-value*	P-value†
Basal					
Anterior	-15.6	-16.5	-17.7	NS	NS
Anteroseptal	-16.4	-18.2	-18.9	NS	NS
Inferoseptal	-13.9	-16.8	-17.5	NS	NS
Inferior	-13.2	-15.9	-17.3	**< 0.05**	NS
Inferolateral	-18.5	-18.2	-20.7	**< 0.05**	NS
Lateral	-17.2	-17.5	-21.2	**< 0.05**	**< 0.05**
Mid					
Anterior	-17.4	-17.7	-19.8	NS	NS
Anteroseptal	-18.5	-19.3	-18.6	NS	NS
Inferoseptal	-17.3	-17.8	-19.1	NS	NS
Inferior	-13.5	-17.0	-19.8	**< 0.05**	NS
Inferolateral	-19.3	-19.1	-22.1	**< 0.05**	NS
Lateral	-19.3	-18.2	-23.0	**< 0.05**	**< 0.05**
Apical					
Anterior	-19.4	-18.6	-21.5	NS	NS
Septal	-17.7	-18.3	-19.3	NS	NS
Inferior	-15.6	-16.7	-19.1	NS	NS
Lateral	-18.8	-18.2	-23.4	**< 0.05**	**< 0.05**

* p-value for comparison between definite ARVD patients and controls

† p-value for comparison between probable ARVD patients and controls